Research Article | Vol. 28, No. 21 / 12 October 2020 / Optics Express 32214
Optics EXPRESS

Recovering cavity effects in corrugated organic light emitting diodes

XIANGYU FU,[1] YI-AN CHEN,[2] DONG-HUN SHIN,[3] YASH MEHTA,[1] I-TE CHEN,[2] NILESH BARANGE,[1] LIPING ZHU,[1] STEPHEN AMOAH,[1] CHIH-HAO CHANG,[2] AND FRANKY SO[1,*]

[1]*Department of Material Science and Engineering, North Carolina State University, Raleigh, NC 27695, USA*
[2]*Walker Department of Mechanical Engineering, University of Texas at Austin, Austin, TX 78712, USA*
[3]*Department of Chemical and Biomolecular Engineering, North Carolina State University, Raleigh, NC 27695, USA*
fso@ncsu.edu

Abstract: Cavity effects play an important role in determining the out-coupling efficiency of an OLED. By fabricating OLEDs on corrugated substrates, the waveguide and SPP modes can be extracted by diffraction. However, corrugation does not always lead to an enhancement in out-coupling efficiency due to the reduction of the electrode reflectance and hence the cavity effects. Based on the results of our rigorous couple-wave analysis (RCWA) simulation, we found that the cavity effects can be partially recovered using a low index Teflon layer inserted between the ITO anode and the substrate due to the enhancement of the reflectance of the corrugated electrodes. To verify the simulation results, we fabricated corrugated OLEDs having a low-index Teflon interlayer with an EQE of 36%, which is 29% higher than an optimized planar OLED. By experimentally measuring the OLED air mode dispersion, we confirm the cavity emission of a corrugated OLED is enhanced by the low index layer.

1. Introduction

OLEDs are great candidates for solid state lighting due to their broad spectrum, simple fabrication, and flexibility [1]. Cavity effects play an important role in determining the out-coupling efficiency, which in turn affects the power consumption and lifetime of OLEDs. By optimizing the cavity effects, the outcoupling efficiency can reach 25% [2,3]. In a typical OLED, over 70% of the light is trapped as the substrate mode, waveguide mode and surface plasmon polariton (SPP) mode, which subsequently dissipates as heat due to absorption [4]. Therefore, improving the outcoupling efficiency of OLEDs has a great implication on energy conservation [5].

One way to extract the trapped light is to fabricate OLEDs on corrugated substrates [6] (Fig. 1). Because the metal cathode and the ITO anodes are corrugated, both waveguide modes and SPP modes can be extracted by scattering [7]. The corrugation pattern is often a periodic or quasi-periodic nano-structure with a feature size close to the wavelength of light [8,9] and the resulting photonic crystals (PhCs) [10] can diffract light coherently towards the normal directions of the substrate, leading to enhancements in outcoupling efficiency [11,12].

While two to three times enhancements in the device efficiency have been reported, the reference planar devices are often not optimized, and the real efficiency enhancement due to corrugation might actually be significantly lower. One of the reasons why corrugation in OLEDs does not always yield enhancement in outcoupling efficiency is due to the loss of cavity effects. In an optimized OLED cavity, photons resonate between a metal electrode and an ITO/glass interface forming cavity modes. In a corrugated OLED, the corrugation at both electrodes reduces their reflectance and results in the loss of cavity effects. As a result, the loss of the cavity

#404412 https://doi.org/10.1364/OE.404412
Journal © 2020 Received 3 Aug 2020; revised 9 Sep 2020; accepted 12 Sep 2020; published 9 Oct 2020

Optics EXPRESS

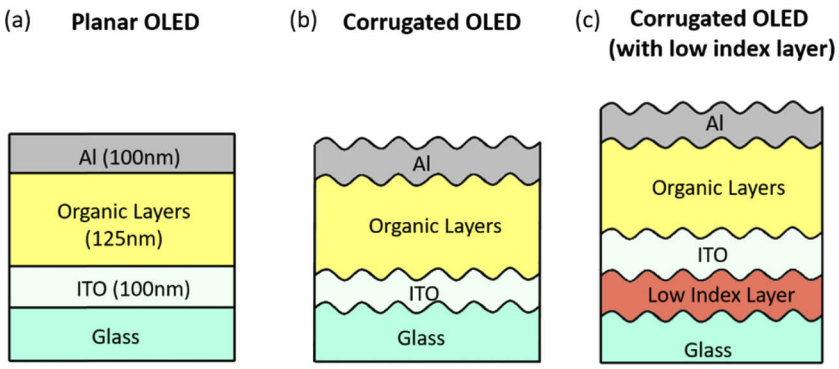

Fig. 1. Schematic drawing of the device structure of (a) a planar OLED, (b) a corrugated OLED and (c) a corrugated OLED with a low index layer inserted between the ITO and glass substrate.

effect might outweigh the gain from the extraction of the waveguide and SPP modes, lowering the overall efficiency of the final corrugated devices.

To understand the effect of corrugation on cavity modes, we conducted RCWA simulation to calculate the reflection and diffraction of the corrugated electrodes. The results show that with a 1-D PhC (grating), the reflection of the Al electrode is reduced by over 50%, while with a 2-D PhC, the reduction is less than 20%. As a result, a 2-D PhC has less impact on the cavity effect. To confirm these findings, we fabricated corrugated OLEDs on 1-D and 2-D PhCs and compared them with an optimized planar OLED having an external quantum efficiency (EQE) of 28%. As expected, the 1-D corrugated OLED yields a slightly lower EQE of 25%, while the 2-D corrugated OLED yields a higher EQE of 32%.

To gain a deeper understanding of the device optics, we used angle-resolved emission spectra (ARES) measurements to experimentally map the OLED mode dispersion, which reveals both cavity modes and extracted trapped modes in the corrugated devices [13,14]. By de-coupling the cavity modes from the extracted modes, we observed a significant suppression of the cavity effect in corrugated OLEDs, with the suppression being stronger in the 1-D PhC device than the 2-D PhC device. Therefore, the loss of the cavity effect outweighs the gain in extracted modes and leads to a lower outcoupling efficiency in 1-D PhC corrugated OLEDs.

Since the reduction of the cavity effects is due to the loss of reflectance at the corrugated electrodes, the out-coupling efficiency can be improved by enhancing the electrode reflectance. Based on the RCWA simulation results, we found that the reflectance of a corrugated ITO interface can be enhanced from 2% to 5% with a low refractive index Teflon layer underneath the ITO electrode, which can in turn recover the cavity effect (Fig. 1(c)). Adopting this strategy, we fabricated corrugated OLEDs with a Teflon layer having an EQE of 36% and achieved a 29% enhancement compared to an optimized planar OLED. The study offers a cost-effective solution to improve the outcoupling efficiency of corrugated OLEDs.

2. Cavity effect in planar OLEDs

Researchers often demonstrate light extraction enhancements of corrugated OLEDs using unoptimized planar OLEDs as a reference, leading to misguiding results. To fully analyze the effect of light extraction in corrugated OLEDs, an in-depth optical characterization is needed. In this study, we first optimize the planar OLED structure by tuning the thickness of the electron transport layer (ETL), then measure the air mode dispersion using ARES. By normalizing the

Optics EXPRESS

air mode dispersion, we found that the cavity mode profile and intensity change with the ETL thickness, and these two factors play a key role in determining the device EQE.

For the reference OLED device, we use the following structure: glass/ITO (110 nm) /MoO_x (5 nm) / 4,4′-Cyclohexylidenebis[N,N-bis(4-methylphenyl)benzenamine] (TAPC) (40 nm) / 4,4′-Bis(N-carbazolyl)-1,1′-biphenyl (CBP) (20 nm): 7% Bis[2-(2-pyridinyl-N)phenyl-C] (acetylacetonato)iridium(III)($Ir(ppy)_2(acac)$) / 4,6-Bis(3,5-di(pyridin-3-yl)phenyl)-2-methylpyrimidine (B3PYMPM) (10 nm) / 4,7-Diphenyl-1,10-phenanthroline (Bphen) (50 nm) / Cs_2CO_3 (2 nm)/ Al (100 nm). Because the hole mobility of CBP is 10 times higher than the electron mobility [15], the emission zone is located at the CBP/B3PYMPM interface, where CBP and B3PYMPM form an exciplex state and transfer energy to the green emitter $Ir(ppy)_2(acac)$ [16]. In addition, $Ir(ppy)_2(acac)$ shows a preferred horizontal dipole ratio of 76% when doped in CBP, which is beneficial for the OLED outcoupling efficiency [17]. The thickness of each layer is optimized using an optical simulation software Setfos, which yields an outcoupling efficiency of 30% (Fig. S1).

To optimize the OLED structure, we fabricated devices with ETL thicknesses of 30 nm, 50 nm, and 70 nm. With these devices, we observed the highest EQE of 28% in the device with a 50 nm thick ETL (Fig. S2). The small difference between the EQE and theoretical outcoupling efficiency is due to non-ideal quantum yield of the emitter and the charge balance factor. For a deeper insight of the optical properties, we characterize the air mode dispersion of the devices by performing ARES measurements (Figs. 2(a)–2(c)). All OLEDs show an intensity maximum at around 2.4 eV, consistent with the electroluminescent (EL) peak of $Ir(ppy)_2(acac)$. Due to the cavity effect, as the ETL thickness increases from 30 nm to 70 nm ETL, the air mode peak shifts from small viewing angles to larger angles; at an ETL thickness of 50 nm, the air mode is noticeably the strongest of the three devices, indicating that the ETL thickness is optimized for the cavity mode.

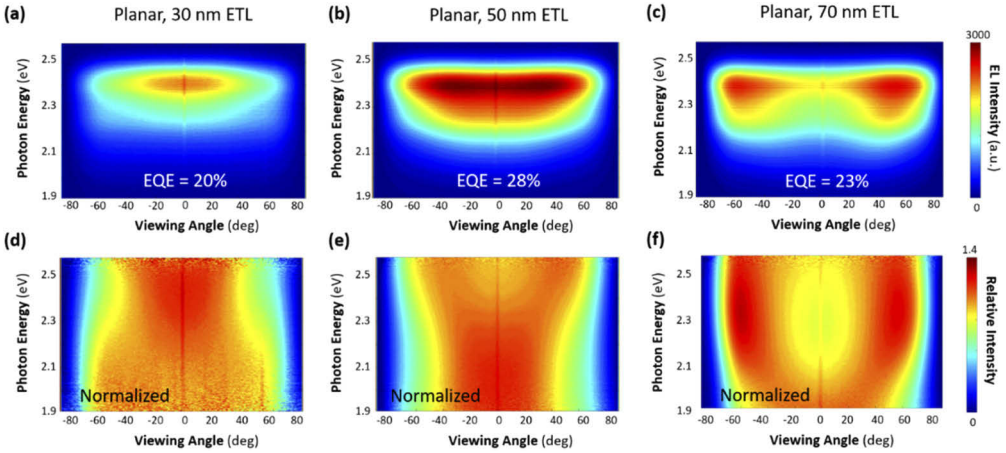

Fig. 2. The measured air mode dispersion of planar OLEDs with (a) 30 nm ETL, (b) 50 nm ETL, (c) 70 nm ETL and (d)-(f) are the corresponding normalized air mode dispersion.

To better visualize the cavity modes, we integrated the photon counts at each wavelength and normalize them to one [14]. The normalization eliminates the effects of the emitter and reveals the optics of the parabolic-shaped cavity modes (Figs. 2(d)–2(f)). As the ETL thickness increases from 30 nm to 70 nm, the cavity length increases, and the cavity mode profile shifts towards lower photon energies (longer wavelengths). The light outcoupling efficiency is partly determined by the overlap between the cavity mode and the emitter spectrum. At an ETL thickness of 30 nm, the distance between the EML and the Al cathode is too small, most of the cavity mode is localized

Optics EXPRESS

at higher photon energies, resulting in a low efficiency. At an ETL thickness of 50 nm, the parabolic shaped emission profile shifts to the EL emission peak at 2.4 eV and light emission from $Ir(ppy)_2(acac)$ is enhanced due to the cavity effects, leading to a high outcoupling efficiency (Fig. S3). At an ETL thickness of 70 nm, the parabolic shaped emission profile shifts downwards past the EL peak. The two cavity mode branches extend outside the air mode, leaving two stripes at large angles. This emission profile indicates the peak cavity emission angle is above the critical angle at the glass/air interface, leading to a strong light trapping in the substrate.

From the discussion above, we confirm that the EQE of an optimized reference planar OLED is due to cavity effects. We emphasize that having a strong overlap between the cavity mode and the emitter spectrum in an optimized device is important for outcoupling efficiency. In the next section, we will study how corrugation affects the cavity mode and hence the out-coupling efficiency.

3. RCWA simulation of corrugated Al

In an optimized planar OLED, over 70% of the emitted light is trapped in the device as the substrate mode, waveguide modes, and SPP mode [18]. Waveguide and substrate modes are caused by the total internal reflection from the organic/ITO layers to the glass, and from the glass to air, respectively. The SPP mode in an OLED is an evanescent wave caused by the excitation of surface charges on the metal cathode [19,20]. In an OLED, corrugation in the device will change the propagation angle of the trapped light through scattering, and light propagating towards the normal direction of the substrate will be extracted. With a periodic PhC structure, both the waveguide and SPP modes will be diffracted based on the Bragg's equation [21].

As we discussed above, while corrugation at the electrode interfaces diffracted waveguide and SPP modes, it also reduces the reflectance of the Al cathode, weakening the cavity effect. For a quantitative study of the process, we simulate the reflection, diffraction, and absorption of the corrugated Al interface using rigorous coupled-wave analysis (RCWA) [22]. In the simulation, light is incident from an organic layer onto a corrugated Al mirror. The corrugation used in the simulation is a grating with a periodicity of 350 nm and a depth of 50 nm, and this corrugation geometry is based on the SEM image of a fabricated corrugated OLED which we will discuss later (Fig. S4).

In Figs. 3(a) and 3(b), we plot the reflection/diffraction efficiencies of a planar mirror and a 1-D corrugated mirror for incident angles between 0° and 90°. Note that the critical angle from the organic layer to air is $\theta_C \sim 34°$, therefore, angles below θ_C contribute to the cavity modes through reflection, and angles above θ_C contribute to the light extraction through diffraction. For the TE light, corrugation reduces the reflectance from 85% to 70%, but gives rise to a 15% diffraction. For the TM light, the reflectance drops to 20%; while 20% of the light is diffracted, and over 20% of the light is still absorbed by the metal. The difference in TE and TM light is caused by the orientation of the grating and the electric field of the incident light. When the grating is rotated 90°, we see a stronger reduction in TE light reflectance instead (Fig. S5).

While the reduction in reflectance is inevitable with a corrugated Al electrode, its amount is a strong function of the corrugation geometry. Based on the Maxwell equations, the change in reflectance with a 1-D PhC is caused by the refractive index modulation along and normal to the grating grooves, which strongly affects the TE light and the TM light, respectively [23]. With a 2-D PhC, the index modulation is within the entire substrate plane, but the high index region and low index region are interconnected, therefore the modulation to the photon electric field is weaker (Fig. S6). This leads to a smaller perturbation to the optical properties of the Al electrode in terms of both the reflectance and diffraction. Figures 3(c) and 3(d) show the simulated reflectance and diffraction of a 2-D PhC with a square lattice and bullet-shaped lattice units. The reflectance with the 2-D PhC is close to 70% for the TE light and 60% for the TM light, which is much higher than the 1-D grating case, indicating that the 2-D PhC has a lower impact

Optics EXPRESS

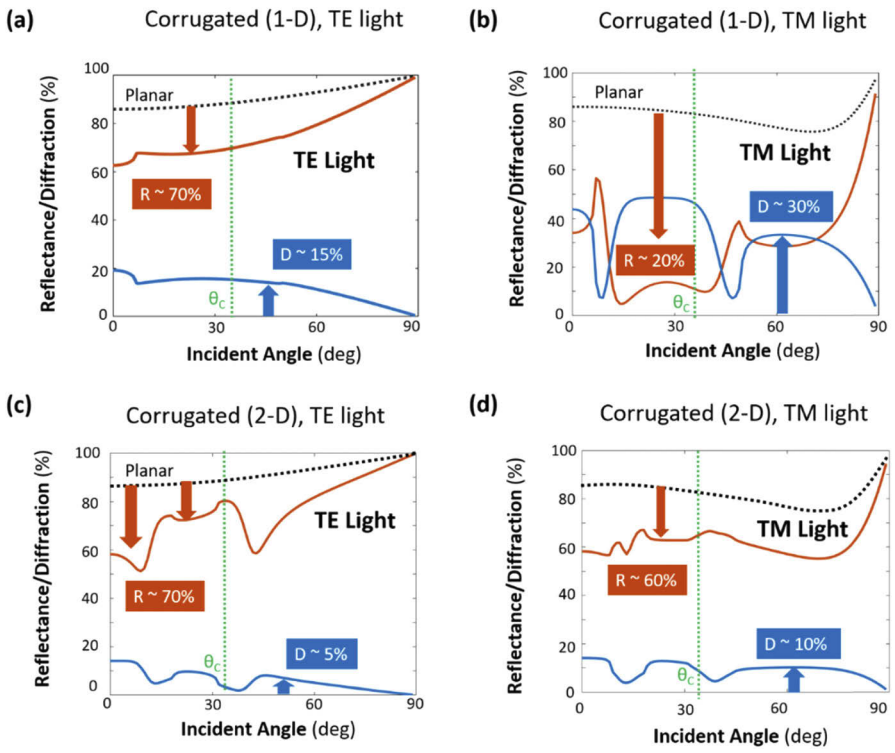

Fig. 3. Reflection and diffraction of (a) TE polarized and (b) TM polarized light from a 1-D corrugated Al mirror coated with an organic layer calculated using RCWA. The reflectance of the planar Al mirror is shown as a reference and (c)-(d) are the same plots for 2-D square-lattice corrugation.

on the OLED cavity mode, while the diffraction efficiency is reduced to 5% for the TE light and 10% for the TM light, suggesting that light diffraction is weaker with a 2-D PhC (Fig. S7).

Based on the discussion above, the outcoupling efficiency of a corrugated OLED is determined by the interplay between the extraction of trapped light and the reduction of cavity emission due to corrugation. With a 1-D grating, we expect stronger light extraction but much reduced cavity effect. With a 2-D PhC, the cavity effect is better preserved, but the extraction of the waveguide and SPP modes might be weakened. In the next section, we will experimentally determine the influence of 1-D and 2-D PhCs on the cavity effect and extracted light using ARES, then correlate the results to the outcoupling efficiency.

4. Corrugated OLEDs on 1-D and 2-D PhCs

We first study the effect of corrugation on the outcoupling efficiency of the 1-D grating device. 1-D grating master molds are fabricated on silicon wafers using a combination of interference lithography (IL) and reactive ion etching (RIE). The grating is then replicated onto a layer of optical adhesive (NOA 81) on the glass substrate. This method yields a smooth 1-D corrugated substrate with a 350 nm period and a 100 nm depth resulting in a bullet-shaped profile (Fig. S4).

We fabricated 1-D corrugated OLEDs using the same organic layers as the planar OLEDs. For comparison, the ETL thickness is varied from 50 nm to 90 nm. The range of ETL we use for the corrugated OLEDs is thicker than the planar OLEDs to reduce the leakage current due to strong localized electric fields [21]. The highest EQE of 25% is achieved with a device having a 70 nm thick ETL compared to an optimum EQE of 28% for the reference OLED (Fig. S8). The different

Optics EXPRESS

optimized ETL thickness indicates the phase relation of the cavity mode in a corrugated OLED is different from the planar OLED, and the lower efficiency implies that the gain in extraction of trapped modes cannot outweigh the loss of the cavity mode due to corrugation.

To confirm our hypothesis, we measured the air mode of the corrugated OLEDs normal to the grating grooves (Figs. 4(a)–4(c)). All three corrugated OLEDs show similar narrow diffraction lines on a diffuse background having different intensities. After normalizing the air mode profile, we can see the diffraction lines are continuous across all wavelengths (Figs. 4(d)–4(f)). Based on the dispersion relation of the diffraction lines, we can calculate the source of the extracted modes using the Bragg equation $\mathbf{k'} = \mathbf{k} + \mathbf{k_G}$, where $\mathbf{k}$ and $\mathbf{k'}$ are the in-plane wavevector of the trapped light and the diffracted light, respectively, and $\mathbf{k_G}$ is the grating vector [14]. By comparing the calculated $\mathbf{k}$ values with the optical simulation in Setfos and subtracting the value of $\mathbf{k_G}$ from the waveguide and SPP trapped modes, the trapped modes are shifted toward the air mode, and hence we can assign the extracted light to the TM waveguide, TE waveguide and SPP modes (Fig. S9). Therefore, the air mode dispersion in corrugated devices is a combination of both the cavity mode and the extracted trapped mode. In the presence of the distinctive diffraction lines, the cavity modes are less intense in the normalized air mode plots.

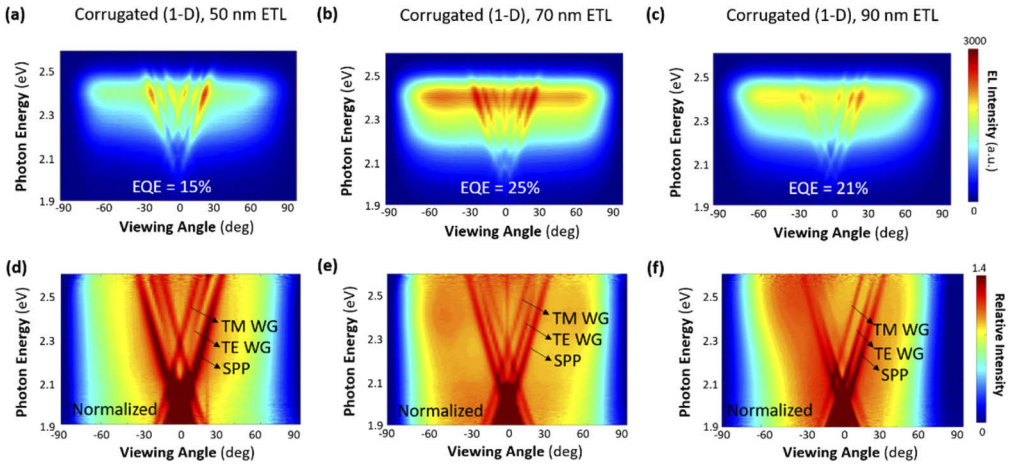

Fig. 4. The measured air mode dispersion of corrugated OLEDs with (a) 50 nm ETL, (b) 70 nm ETL, (c) 90 nm ETL and (d)-(f) are the corresponding normalized air mode dispersion plots.

To correlate the efficiency with the cavity modes and the extracted modes, we need to de-couple the sharp diffraction lines from the broad diffuse background. Schwab *et al.* has shown that the angular emission from a thin film cavity can be fitted by Lorentz-like resonances [24]. Using a similar method, we estimate the background using polynomial functions with an order up to 8 (see Section 6). As a result, the diffraction lines are extracted from the background, which allows us to compare the diffuse background and the extracted light separately (Figs. 5(a)–5(c)). Here, we can assign the diffraction features as the extracted waveguide and SPP modes and the diffuse background as the residual cavity mode in the corrugated device. At an ETL thickness of 50 nm ETL, the background emission profile is similar to that of the planar OLED having a 30 nm thick ETL, with light emission in the normal direction being the strongest. At an ETL thickness of 70 nm, the background intensity is the strongest compared to the other two devices, with an intensity maximum at the air mode center and two less noticeable maxima at ± 60° viewing angles. At an ETL thickness of 90 nm, the background intensity is reduced again, showing two maxima at ± 50° viewing angles. In all three cases, the diffuse background has a different

Optics EXPRESS

dispersion and lower intensity compared to the planar OLEDs with the same ETL thickness, indicating the corrugation does suppress the cavity effect and reduces its emission intensity.

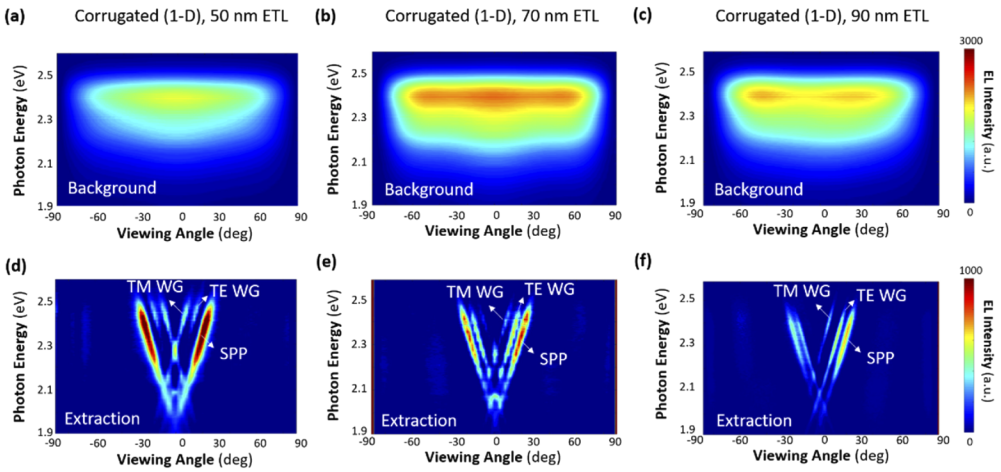

Fig. 5. The processed air mode dispersion of corrugated OLEDs by separating (a)(b)(c) the cavity emission ('background') and (d)-(f) the diffraction peaks ('extraction') at 50 nm, 70 nm and 90 nm ETL, respectively.

Figures 5(d)–5(f) show the profile of the extracted optical modes for devices with different ETL thicknesses. From the data, increasing the ETL thickness does lower the intensity of the extracted modes. This reduction in extracted modes is due to the reduction of the corrugation depth on the Al cathode as a result of the thermal evaporation [25]. Evaporating OLED layers on a corrugated surface will partially planarize the corrugation, and as a result increasing the ETL thickness will reduce the corrugation at the Al electrode leading to weaker diffraction. It is obvious that the intensity of the extracted modes is the strongest for the 50 nm thick ETL device and decreases with an increasing ETL thickness. On the other hand, the intensity of the cavity mode is the strongest for the 70 nm thick ETL device, which indicates the cavity effect is optimized at this ETL thickness for the corrugated OLED. Therefore, the overall device outcoupling efficiency is determined by the combination of the intensity of the cavity mode as well as the waveguide and SPP modes, and the gain in extracted mode does not outweigh the loss in the cavity mode.

To gain a more in-depth understanding of the optics of corrugated OLEDs, we also fabricate 2-D corrugated OLEDs using a polycrystalline PhC (poly-PhC). A poly-PhC is a quasi-periodic pattern that has a short-range order of hexagonal close-packed lattice but lacking a long-range order. The poly-PhC is chosen for the 2-D corrugated OLED because its isotropic light emission in the in-plane direction, an essential feature for lighting applications.

We first fabricated a poly-PhC master mold using a combination of colloidal assembly and RIE [26,27]. The colloidal assembly module consists of a Langmuir-Blodgett trough, where colloidal nanospheres (390 ± 10 nm diameter) self-assemble into a monolayer of hexagonal closed-packed lattice on the surface of fluid. By controlling the nanosphere flow rate on a silicon wafer, the nanospheres can form quasi-periodic grains on the order of microns size (Fig. S10). The wafer is etched by RIE using the nanosphere array as the mask. By controlling the etching conditions, we obtained a corrugated pattern with a depth of 100 nm, similar to that of the 1-D grating. Using a nanoimprinting process to fabricate corrugated substrates, OLEDs are fabricated on poly-PhC substrates using the beforementioned OLED stack with a 70 nm ETL.

We compare the J-V and EQE characteristics of the corrugated devices with the optimized planar OLED (Fig. 6). The corrugated OLED has a slightly increased current density because of

Optics EXPRESS

the increased electric field due to the corrugated ITO and Al electrodes. The EQE of 32% for the corrugated OLED is higher than the EQE of 28% for the planar OLED. Because the devices show very similar J-V curves and efficiency roll-off, we conclude the enhancement in efficiency is mainly coming from the change in the device optics.

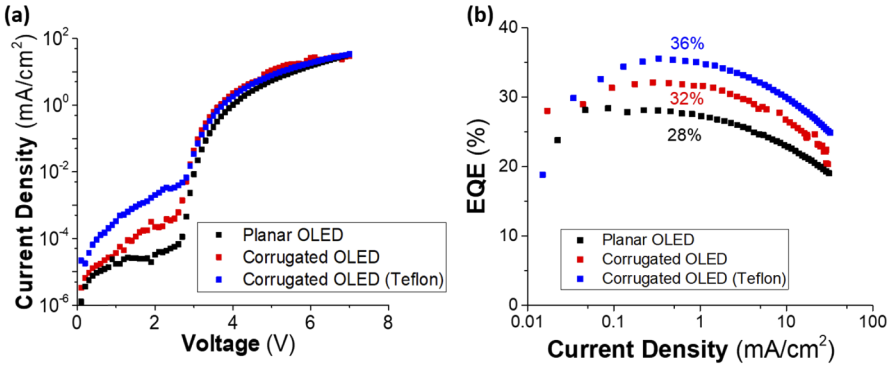

Fig. 6. (a) J-V and (b) EQE comparison of the planar OLED, corrugated OLED and corrugated OLED with a low index Teflon layer. The corrugated substrate has a 2-D poly-PhC pattern.

Figure 7 shows the measured air mode dispersion of the corrugated OLED along with the dispersion of the de-coupled cavity emission and extracted modes. Compared to the 1-D corrugated OLED (Fig. 5(b)), the 2-D corrugated OLED shows noticeably stronger background diffuse emission. The stronger cavity mode in the 2-D device is consistent with our RCWA simulation results that the reflectance of the 2-D PhC is higher than that of the 1-D PhC. From the de-coupled light extraction profile, we observe strong TE waveguide mode peaks but vanishing of diffraction signals due the TM waveguide and SPP modes. This is likely caused by the low diffraction from the corrugated Al with a 2-D PhC. We note that some of the extracted light can contribute to the background emission as well. For example, the substrate mode can be scattered by the corrugation, and the waveguide and SPP modes can be randomly scattered by the grain boundaries of a poly PhC. In either case, the trapped light is scattered to a broad range of angles, blending in with the cavity emission background. Overall, the outcoupling efficiency of the corrugated OLED is 14% higher than that of an optimized planar OLED.

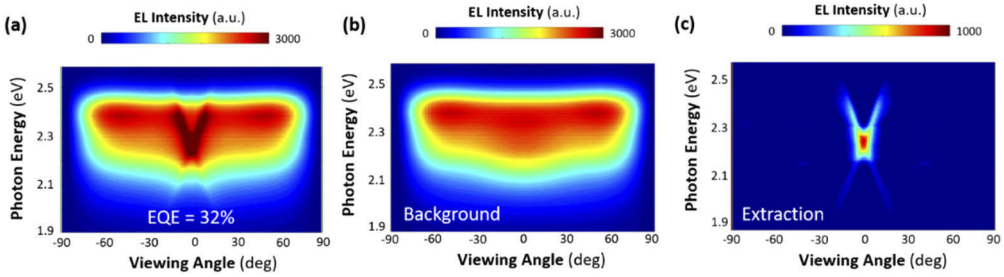

Fig. 7. Measured (a) air mode dispersion of a 2-D corrugated OLED with poly-PhC corrugation. The processed (b) background emission and (c) extraction peaks.

In summary, we fabricated 1-D PhC OLEDs with varied ETL thicknesses, but the efficiency is lower than that of the optimized planar OLED. By measuring the air mode dispersion and de-couple the cavity emission and the extracted light, we confirm the lowered efficiency is caused by a significant reduction of the cavity mode. With a 2-D PhC, the cavity mode is stronger

Optics EXPRESS

than with a 1-D PhC, consistent with the results from RCWA simulation. However, despite the enhancement in the outcoupling efficiency, the cavity background emission of a 2-D corrugated OLED is still lower than the cavity mode of an optimized planar OLED (Fig. 2(b)). In the next section, we aim at recovering the cavity effect in a corrugated OLED with a low index layer.

5. Corrugated OLEDs with a low index layer

Based on the discussion in Section 4, we concluded a lower Al cathode reflectance leads to weaker cavity resonance and hence a lower outcoupling efficiency in a corrugated OLED. However, given the corrugated nature of the Al electrode, it is difficult to further improve its reflectance. Nonetheless, we can recover the cavity effect by increasing the reflectance of the ITO anode (R_{ITO}). From the Fresnel's equation, R_{ITO} is determined by the index contrast at the ITO electrode interfaces with the organic layer and the glass substrate. Based on the refractive indices of organic, ITO and glass: n(organic) ~ 1.8, n(ITO) ~ 2, and n(glass) ~ 1.5, R_{ITO} is around 2%, mainly determined by the index contrast at the ITO/glass interface. To increase the index contrast and hence R_{ITO}, we can add a low index buffer layer (n_{Low}) between the ITO electrode and the glass substrate. Although there has been report of air tunnels built under an ultra-thick ITO anode based on a similar theory, the structure requires solution processing and the air tunnel has limited coverage [28]. In this research, we use Teflon AF 1600 from Chemours Co. since it has a low refractive index of 1.3 at 520 nm and can be thermally evaporated, which is compatible with OLED fabrication [29].

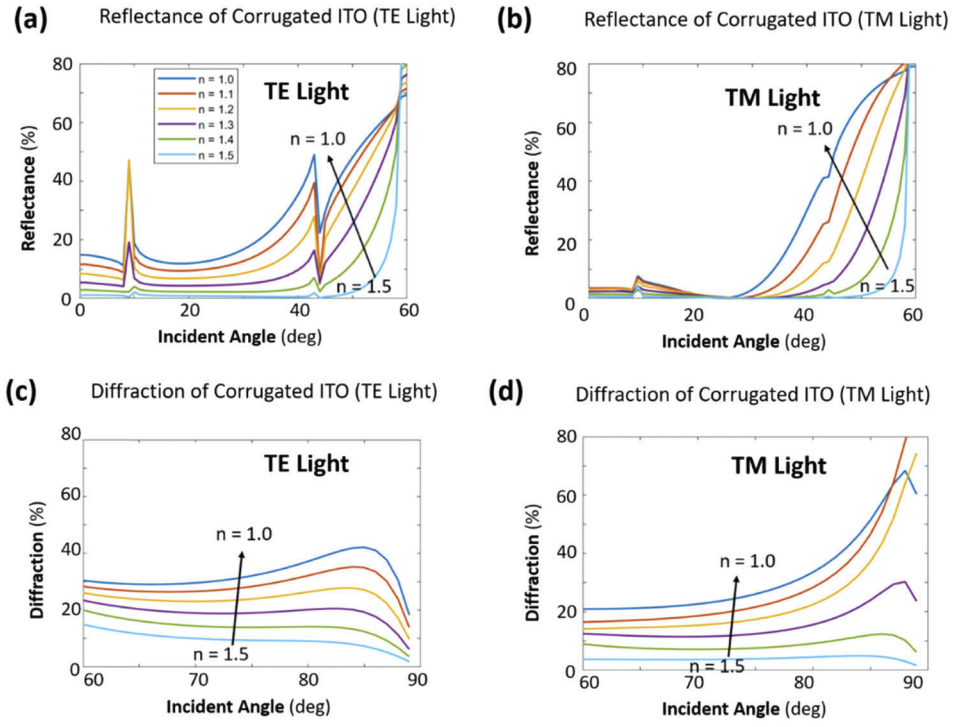

Fig. 8. Simulated (a)-(b) reflection and (c)-(d) diffraction at the corrugated ITO surface in both TE and TM polarizations by varying the refractive index of the low index layer. Both transmitted and reflected diffractions are taken into consideration. The angle ranges of the reflection and diffraction plots are divided by the critical angle from ITO to glass (60°).

Optics EXPRESS

First, we simulate R_{ITO} of a glass/100 nm thick low index layer /ITO structure using RCWA (Figs. 8(a) and 8(b)). The period and depth of the corrugation is 350 nm and 100 nm, respectively. When n_{Low} is reduced to 1.3, R_{ITO} is enhanced from 2% to 5% at angles below θ_C. The higher reflectance results in enhanced cavity resonance and improved outcoupling efficiency. Furthermore, having a low index layer also increases the diffraction of the TE waveguide modes from the corrugated ITO electrode, enhancing the extraction efficiency of the waveguide modes (Figs. 8(c) and 8(d)). With both merits combined, we expect the Teflon-coated corrugated OLED to have improved efficiency compared to the corrugated device without a low index layer.

To demonstrate the effect of a low index layer on the cavity effect and light extraction, we coated the corrugated substrates with a 100 nm thick Teflon AF 1600 film, then deposited the OLED stack on top. We compare the J-V and EQE performance of the planar OLED and corrugated OLED in Fig. 6. With a low index Teflon layer between the glass substrate and the ITO electrode, the EQE of the corrugated OLED is improved to 36%, 12% higher than the 2D corrugated OLED without the low index layer, and 29% higher than an optimized planar OLED.

To analyze the optical modes in the device with a low index buffer layer, we plot the air mode dispersion of a corrugated OLED with a low index Teflon coating in Fig. 9. From the cavity emission background, we can see the Teflon layer significantly enhances the cavity emission, which is represented as a stronger cavity mode peak at ± 55° and stronger cavity mode dispersion curves. In addition, the enhanced index contrast leads to slightly stronger diffraction features, contributing the overall efficiency enhancement.

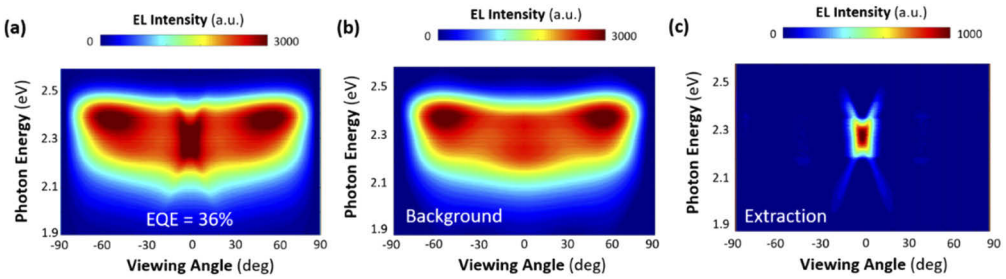

Fig. 9. Measured (a) air mode dispersion of a 2-D corrugated OLED with poly-PhC corrugation and low index Teflon coating. The processed (b) background emission and (c) extraction peaks.

We can also observe the enhanced cavity effect by comparing the air mode in TE and TM polarizations. From the RCWA results in Fig. 3 and Fig. 8, we note the reflectance from Al and ITO is stronger for the TE polarized light than the TM polarized light. Therefore, we expect to see a stronger cavity effect from the TE polarized light. This is tested by measuring the air mode dispersion of the corrugated OLEDs with a linear polarizer. In the regular corrugated OLED, we can see two weak peaks corresponding to the cavity modes in the TE light and almost no peaks in the TM light (Fig. S11). After inserting a low index layer, the TE light cavity mode peaks become much stronger, which confirms the cavity effect is improved by the higher reflectance (Fig. S12).

To quantify the enhancement amount, we integrate the photon numbers with the solid angle term $2\pi sin\theta d\theta$, then the integral should be proportional to the EQE values [30]. Compared with the planar device, we found that the Teflon coating enhances the cavity emission of the corrugated OLED by 16% and light extraction of the trapped modes by 10%, resulting in an EQE of 36%. Based on the results, we confirm the low index Teflon layer enhances the outcoupling efficiency of a corrugated OLED by improving the cavity effect and light extraction. In the corrugated OLEDs we studied, an increase in the index contrast at the ITO electrode leads to an efficiency improvement of 12%.

Optics EXPRESS

6. Methods

6.1. De-coupling of the cavity emission and extracted modes

The air mode dispersion of a corrugated OLED consists of both the diffusive cavity emission background ('Background'), and the narrow diffraction lines from the extracted waveguide and SPP modes ('Extraction'). Because the waveguide and SPP modes are confined in the organic thin films, their mode dispersion is quantized with very narrow line-width. In contrast, the cavity effect in an OLED is weak because of the highly transparent ITO anode, therefore, the background emission is broad and Lambertian-like. This allows us to estimate the Background with low-order polynomials and separate the Extraction from the Background. We used a MATLAB function developed by Mazet *et al.* (https://www.mathworks.com/matlabcentral/fileexchange/27429-background-correction) [31]. A highest polynomial order of 8 is used, and the threshold is tuned to separate the Background from the Extraction with the least overlapping.

7. Conclusion

In summary, we studied the outcoupling efficiency of planar and corrugated OLEDs by experimentally measuring the air mode dispersion and correlating the data with the device efficiency. We first optimized the cavity mode of a planar OLED by varying the ETL thickness, then explained the shift of cavity modes in the normalized air mode and its influence on the OLED performance. We then used RCWA simulation to confirm that corrugation reduces the reflectance of the Al electrode, which in turn weakens the cavity effect in a corrugated OLED, and the reduction of the cavity effects is more detrimental with a 1-D PhC than a 2-D PhC. To verify the theory, we fabricated corrugated OLEDs on both 1-D PhCs and 2-D poly-PhCs and observed a higher efficiency in the 2-D corrugated OLEDs. By de-coupling the cavity emission background and the extracted light from the air mode dispersion, we confirm the improved efficiency is an interplay between the extraction of trapped modes and the reduced cavity mode.

To recover the cavity effect, we inserted a low index Teflon layer beneath the ITO anode which increased its reflectance from 2% to 5%. The corresponding corrugated OLED shows a stronger cavity mode and a 29% higher outcoupling efficiency than that of an optimized planar OLED. The work shows the importance of cavity mode in nanostructured OLED and how to regain the cavity mode by using a low index Teflon layer to enhance the index contrast.

Funding

U.S. Department of Energy (DE-FOA-0001823).

Disclosures

The authors declare no conflict of interest.

See Supplement 1 for supporting content.

References

1. S. Reineke, F. Lindner, G. Schwartz, N. Seidler, K. Walzer, B. Lüssem, and K. Leo, "White organic light-emitting diodes with fluorescent tube efficiency," Nature **459**(7244), 234–238 (2009).
2. R. Meerheim, M. Furno, S. Hofmann, B. Lüssem, and K. Leo, "Quantification of energy loss mechanisms in organic light-emitting diodes," Appl. Phys. Lett. **97**(25), 253305 (2010).
3. J. Ye, C. J. Zheng, X. M. Ou, X. H. Zhang, M. K. Fung, and C. S. Lee, "Management of singlet and triplet excitons in a single emission layer: a simple approach for a high-efficiency fluorescence/phosphorescence hybrid white organic light-emitting device," Adv. Mater. **24**(25), 3410–3414 (2012).
4. A. Salehi, X. Y. Fu, D. H. Shin, and F. So, "Recent advances in OLED optical design," Adv. Funct. Mater. **29**(15), 1808803 (2019).

Optics EXPRESS

5. J. Song, H. Lee, E. G. Jeong, K. C. Choi, and S. Yoo, "Organic light-emitting diodes: pushing toward the limits and beyond," Adv. Mater. **32**(35), 1907539 (2020).
6. D. Yin, J. Feng, R. Ma, Y. F. Liu, Y. L. Zhang, X. L. Zhang, Y. G. Bi, Q. D. Chen, and H. B. Sun, "Efficient and mechanically robust stretchable organic light-emitting devices by a laser-programmable buckling process," Nat. Commun. **7**(1), 11573 (2016).
7. P. A. Will, E. B. Schwarz, C. Fuchs, R. Scholz, S. Lenk, and S. Reineke, "Scattering quantified: Evaluation of corrugation induced outcoupling concepts in organic light-emitting diodes," Org. Electron. **58**, 250–256 (2018).
8. H. Liang, H.-C. Hsu, J. Wu, X. He, M.-K. Wei, T.-L. Chiu, C.-F. Lin, J.-H. Lee, and J. Wang, "Corrugated organic light-emitting diodes to effectively extract internal modes," Opt. Express **27**(8), A372–A384 (2019).
9. H. Liang, R. Zhu, Y. Dong, S.-T. Wu, J. Li, J. Wang, and J. Zhou, "Enhancing the outcoupling efficiency of quantum dot LEDs with internal nano-scattering pattern," Opt. Express **23**(10), 12910–12922 (2015).
10. E. Yablonovitch, "Photonic band-gap structures," J. Opt. Soc. Am. B **10**(2), 283 (1993).
11. Q. D. Ou, L. Zhou, Y. Q. Li, S. Shen, J. De Chen, C. Li, Q. K. Wang, S. T. Lee, and J. X. Tang, "Extremely efficient white organic light-emitting diodes for general lighting," Adv. Funct. Mater. **24**(46), 7249–7256 (2014).
12. H. Fujimoto, M. Yahiro, T. Kawashima, K. Konno, Q. Chen, K. Sawaya, S. Kawakami, and C. Adachi, "Improvement in the light outcoupling efficiency of organic light-emitting diodes using a hemispherical lens and a multipatterned one-dimensional photonic crystal fabricated by autocloning," Appl. Phys. Express **8**(8), 082102 (2015).
13. J. J. Wierer, A. David, and M. M. Megens, "III-nitride photonic-crystal light-emitting diodes with high extraction efficiency," Nat. Photonics **3**(3), 163–169 (2009).
14. X. Y. Fu, C. Peng, M. Samal, N. Barange, Y. A. Chen, D. H. Shin, Y. Mehta, A. Rozelle, C. H. Chang, and F. So, "Mode dispersion in photonic crystal organic light emitting diodes," ACS Appl. Electron. Mater. **2**(6), 1759–1767 (2020).
15. J. W. Kang, S. H. Lee, H. D. Park, W. I. Jeong, K. M. Yoo, Y. S. Park, and J. J. Kim, "Low roll-off of efficiency at high current density in phosphorescent organic light emitting diodes," Appl. Phys. Lett. **90**(22), 223508 (2007).
16. Y. S. Park, W. I. Jeong, and J. J. Kim, "Energy transfer from exciplexes to dopants and its effect on efficiency of organic light-emitting diodes," J. Appl. Phys. **110**(12), 124519 (2011).
17. C. Y. Lu, M. Jiao, W. K. Lee, C. Y. Chen, W. L. Tsai, C. Y. Lin, and C. C. Wu, "Achieving above 60% external quantum efficiency in organic light-emitting devices using ITO-free low-index transparent electrode and emitters with preferential horizontal emitting dipoles," Adv. Funct. Mater. **26**(19), 3250–3258 (2016).
18. W. Brütting, J. Frischeisen, T. D. Schmidt, B. J. Scholz, and C. Mayr, "Device efficiency of organic light-emitting diodes: Progress by improved light outcoupling," Phys. Status Solidi A **210**(1), 44–65 (2013).
19. W. L. Barnes, A. Dereux, and T. W. Ebbesen, "Surface plasmon subwavelength optics," Nature **424**(6950), 824–830 (2003).
20. H. Liang, Z. Luo, R. Zhu, Y. Dong, J.-H. Lee, J. Zhou, and S.-T. Wu, "High efficiency quantum dot and organic LEDs with a back-cavity and a high index substrate," J. Phys. D. Appl. Phys. **49**(14), 145103 (2016).
21. S. M. Jeong, F. Araoka, Y. Machida, Y. Takanishi, K. Ishikawa, H. Takezoe, S. Nishimura, and G. Suzaki, "Enhancement of light extraction from organic light-emitting diodes with two-dimensional hexagonally nanoimprinted periodic structures using sequential surface relief grating," Jpn. J. Appl. Phys. **47**(6), 4566–4571 (2008).
22. A. C. Wei and J. R. Sze, "Modeling OLED lighting using Monte Carlo ray tracing and rigorous coupling wave analyses," Opt. Commun. **380**, 394–400 (2016).
23. E. Matioli, S. Brinkley, K. M. Kelchner, Y. Hu, S. Nakamura, S. Denbaars, J. Speck, and C. Weisbuch, "High-brightness polarized light-emitting diodes," Light: Sci. Appl. **1**(8), e22 (2012).
24. T. Schwab, C. Fuchs, R. Scholz, A. Zakhidov, K. Leo, and M. C. Gather, "Coherent mode coupling in highly efficient top-emitting OLEDs on periodically corrugated substrates," Opt. Express **22**(7), 7524–7537 (2014).
25. P. A. Will, M. Schmidt, K. Eckhardt, F. Wisser, S. Lenk, J. Grothe, S. Kaskel, and S. Reineke, "Efficiency of light outcoupling structures in organic light-emitting diodes: 2D TiO2 array as a model system," Adv. Funct. Mater. **29**(20), 1901748 (2019).
26. W. Youn, J. Lee, M. Xu, R. Singh, and F. So, "Corrugated sapphire substrates for organic light-emitting diode light extraction," ACS Appl. Mater. Interfaces **7**(17), 8974–8978 (2015).
27. W. H. Koo, Y. Zhe, and F. So, "Direct fabrication of organic light-emitting diodes on buckled substrates for light extraction," Adv. Opt. Mater. **1**(5), 404–408 (2013).
28. Y. S. Shim, J. H. Hwang, C. H. Park, S. G. Jung, Y. W. Park, and B. K. Ju, "An extremely low-index photonic crystal layer for enhanced light extraction from organic light-emitting diodes," Nanoscale **8**(7), 4113–4120 (2016).
29. B. Wang, J. S. Price, and N. C. Giebink, "Durable broadband ultralow index fluoropolymer antireflection coatings for plastic optics," Optica **4**(2), 239–242 (2017).
30. S. Hofmann, M. Thomschke, P. Freitag, M. Furno, B. Lüssem, and K. Leo, "Top-emitting organic light-emitting diodes: Influence of cavity design," Appl. Phys. Lett. **97**(25), 253308 (2010).
31. V. Mazet, C. Carteret, D. Brie, J. Idier, and B. Humbert, "Background removal from spectra by designing and minimising a non-quadratic cost function," Chemom. Intell. Lab. Syst. **76**(2), 121–133 (2005).